ACS OMEGA

Article

http://pubs.acs.org/journal/acsodf

Extending the Scope of a New Cyanation: Design and Synthesis of an Anthracene Derivative with an Exceptionally Low LUMO Level and Improved Solubility

Florian Glöcklhofer,*[,†] Andreas J. Morawietz,[†] Berthold Stöger,[‡] Miriam M. Unterlass,[§] and Johannes Fröhlich[†]

[†]Institute of Applied Synthetic Chemistry, TU Wien, Getreidemarkt 9/163, 1060 Vienna, Austria

[‡]Institute of Chemical Technologies and Analytics, TU Wien, Getreidemarkt 9/164, 1060 Vienna, Austria

[§]Institute of Materials Chemistry, TU Wien, Getreidemarkt 9/165, 1060 Vienna, Austria

Supporting Information

ABSTRACT: The preparation of cyanated acenes from quinones has been improved for the conversion of electron-poor starting materials. The new procedure was used to prepare rationally designed 2,7-dinitro-9,10-dicyanoanthracene. Crystallographic, morphological, and electrochemical investigations have revealed most promising properties for applications in organic electronics.

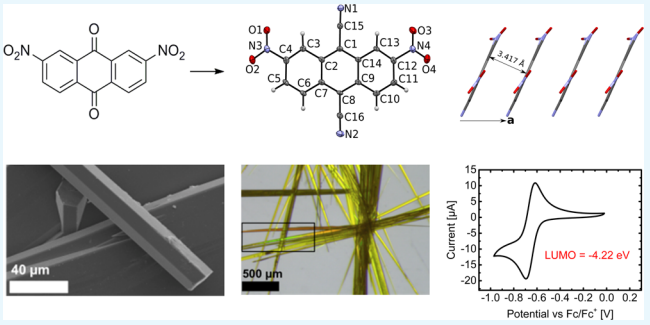

INTRODUCTION

Electron-withdrawing groups (EWGs) can be introduced to efficiently modify the properties of organic compounds.[1,2] The highest occupied molecular orbital (HOMO) and the lowest unoccupied molecular orbital (LUMO) levels are lowered by these groups, resulting in electron-poor materials, which are useful for various applications ranging from n-type transistors to rechargeable batteries.[3]

Attaching two or more cyano groups to acenes has been found to be a particularly useful strategy. Cyano groups exhibit large electron-withdrawing effects and additionally favor a dense, face-to-face molecular packing,[4−7] which is of utmost importance for efficient charge transport in organic materials.[1,2,8] Moreover, the cyano group is thermally very stable, enabling material processing at elevated temperatures.

A low-cost one-pot synthesis, which has been developed in our group, allows for a straightforward preparation of such cyanated acenes from quinones in two steps (Scheme 1).[4,7,9,10] In the first step of the synthesis, the carbonyl groups are converted into silylated cyanohydrins using trimethylsilyl cyanide (TMSCN) and a cyanide salt catalyst such as KCN. In the second step, PBr_3 is added for the reductive aromatization, yielding the cyanated acenes. 6,13-Dicyanopentacene and 5,7,12,14-tetracyanopentacene have been recently prepared by this reaction.[7] Both compounds exhibit very low LUMO levels, enabling electron transport in organic thin-film transistors even under ambient conditions. However, the solubility of these cyanated pentacenes is very low, rendering their purification by flash chromatography difficult and processing from solution impossible.

Scheme 1. One-Pot Synthesis of Cyanated Acenes from Quinones in Two Steps via Silylated Cyanohydrin Intermediates

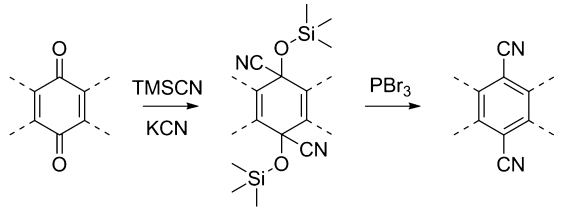

The solubility of acenes depends not only on the functional groups but also on the size of the aromatic π-system.[11] Shrinking the size of acenes improves their solubility. Unfortunately, a smaller π-system also results in higher LUMO levels.[12] An increased number of EWGs per ring is required to compensate this effect. Attaching two additional cyano groups to the well-investigated 9,10-dicyanoanthracene (DCA) may appear as a reasonable approach; a straightforward synthesis of such tetracyanoanthracenes has been reported.[13] However, these compounds do not exhibit satisfying solubility despite the smaller aromatic π-system. Attaching alkylated

Received: March 2, 2017
Accepted: April 10, 2017
Published: April 24, 2017

DOI: 10.1021/acsomega.7b00245
ACS Omega 2017, 2, 1594−1600

Scheme 2. Synthesis of 2,7-Dinitro-9,10-dicyanoanthracene 2 (with a Supposed Mechanism); Reduction to Diamine 3; Formation of Halogenated Byproduct 4, *Calculated Yield (2 Contaminated with 1 and 4)

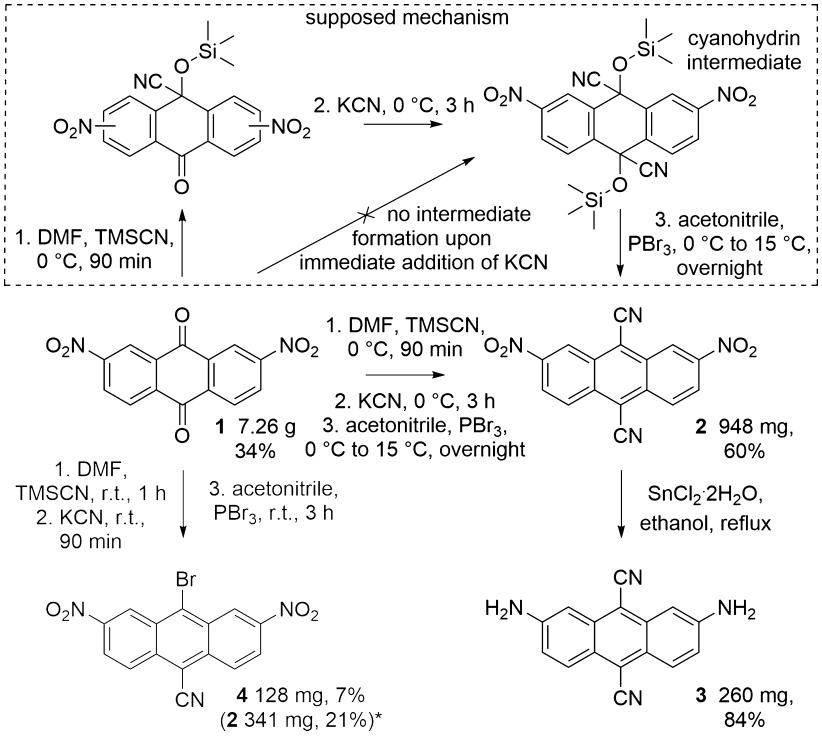

electron-withdrawing groups, such as imides, improves the solubility,[14] but the insulating alkyl chains can deteriorate the charge transport properties.[15]

RESULTS AND DISCUSSION

The aim of this work was to develop an anthracene derivative with a similarly low LUMO level as the cyanated pentacenes but with improved solubility (despite avoiding functionalization with insulating alkyl chains). Therefore, we developed the idea of attaching two nitro groups to DCA. Similar to the cyano group, the nitro group is known for its strong electron-attracting power and can change the electron affinity of molecules significantly,[16] which is most promising for low LUMO levels. In addition, the nitro group exhibits a more complex geometry (V-shaped) than the cyano group (linear), which is expected to result in increased solubility. Moreover, the nitro group is typically a weaker H-bond acceptor, which is also expected to improve the solubility. In a similar approach, we could significantly enhance the solubility of dicyanoanthracene precursors for coupling reactions.[10] As an additional advantage, the reduction of the nitro groups to amines opens a pathway to cyanated anthracenes with amino substituents, which may allow for further modifications by chemical reactions.

The synthesis of cyanated acenes developed in our group can be used to introduce the cyano groups in the 9,10-position of anthracene (Scheme 2). The nitro groups were placed in the 2,7-position for two reasons. First, the absence of a center of inversion in the resulting molecular structure is expected to improve the solubility by decreased symmetry;[17] second, the required 2,7-dinitroanthraquinone precursor, **1**, is easily accessible from anthrone on a multigram scale.[18]

However, carrying out the conversion of **1** into 2,7-dinitro-9,10-dicyanoanthracene **2** turned out to be more challenging than expected. The reaction immediately turned black when the KCN catalyst was added to **1** in DMF; no formation of the cyanohydrin intermediate was observed. Luckily, carrying out the reaction in three steps instead of two (by delayed addition of the catalyst) yielded better results (Scheme 2, supposed mechanism). We suppose that the electron-poor character of **1** enables the formation of one cyanohydrin per molecule without the catalyst (step 1). This catalyst-free reaction reduces the electron-poor character of the molecule, which prohibits the formation of the second cyanohydrin. However, after this first step, it is possible to add the catalyst without unwanted reactions, enabling the second cyanohydrin to be formed (step 2). Carrying out these steps at 0 °C and using KCN as the catalyst, full conversion to the cyanohydrin intermediate was achieved.

Target compound **2** was formed in the third step without optimization of the reaction conditions, but back-formation of **1** was observed; **1** and **2** could not be separated by column chromatography. Moreover, significant amounts of a less polar byproduct were formed. On the basis of NMR measurements, we assumed the formation of halogenated compound **4** (Scheme 2). X-ray diffraction confirmed this assumption (see Supporting Information (SI); single crystals grown from $CDCl_3$). Interestingly, the formation of this byproduct is pointing the way for a synthesis of halogenated acenes by reductive aromatization. As a possible mechanism, we propose that the addition of PBr_3 results in the substitution of the intermediate *O*-silyl group by bromide, which is then followed by reductive aromatization.

The formation of **4** and the back-formation of **1** were efficiently suppressed by keeping the temperature at 0 °C overnight using a cryostat. For an optimized preparation on a larger scale, we successfully carried out the reductive aromatization in an ice-filled, covered Dewar flask without a

DOI: 10.1021/acsomega.7b00245
ACS Omega 2017, 2, 1594−1600

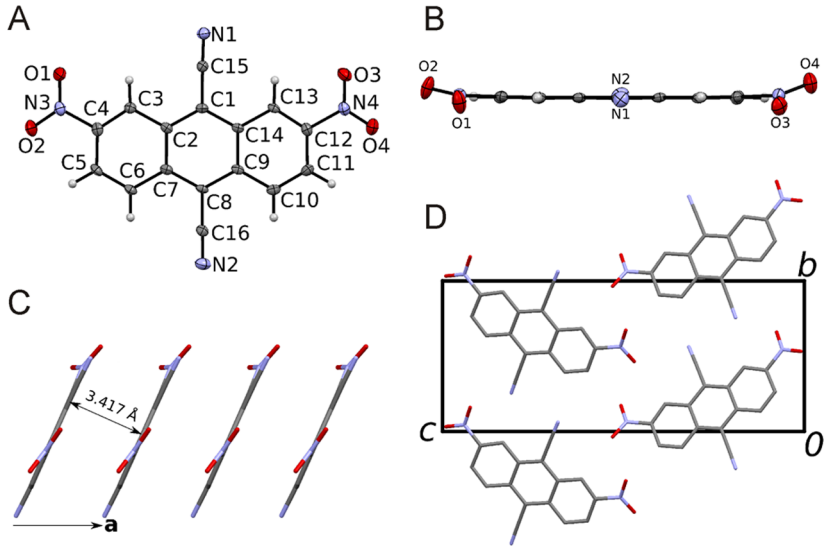

Figure 1. (A, B) Molecular structure of **2**; ellipsoids drawn at the 50% probability levels, H atoms represented by white spheres of arbitrary radius. (C) Rods of **2** connected by $\pi-\pi$ interactions. (D) Crystal structure of **2** viewed down [100]; H atoms omitted for clarity.

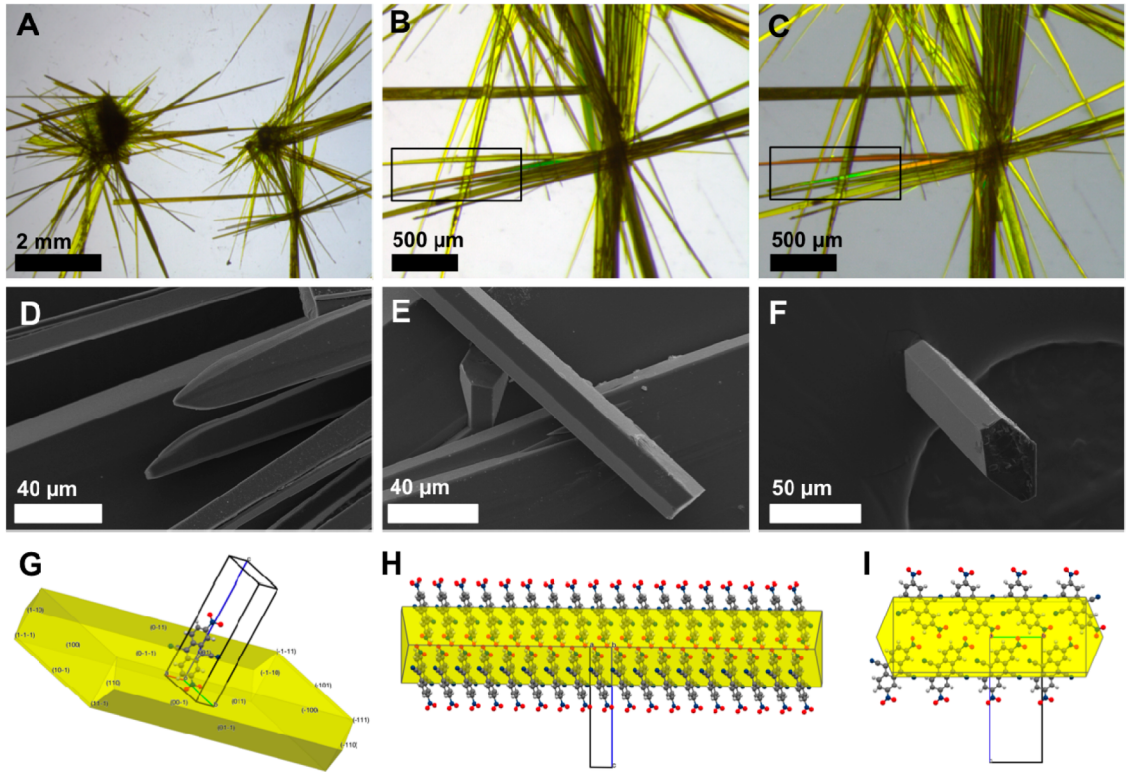

Figure 2. Optical micrographs (top), SEM images (middle), and Bravais–Friedel–Donnay–Harker (BFDH)-predicted morphology (bottom) of single crystals of **2**. Overview image (A) and details at higher magnification (B, C) with the polarization filter turned by 90° (C); boxes highlight pleochroism (B, C).

cryostat. Although the reaction was not kept at 0 °C overnight, yields of 60% were obtained for **2** by this approach.

As expected, **2** showed good solubility in various polar solvents, such as acetonitrile (1.5 g·L^{-1}), nitromethane (3.7 g·L^{-1}), $CHCl_3$ (1.8 g·L^{-1}), and CH_2Cl_2 (4.0 g·L^{-1}), in contrast to the cyanated pentacenes (6,13-dicyanopentacene: 200 mg·L^{-1} in CH_2Cl_2, 5,7,12,14-tetracyanopentacene: 60 mg·L^{-1} in CH_2Cl_2).[7] The selective reduction of the nitro groups was demonstrated by the preparation of diamine **3** using $SnCl_2$ as the reagent (Scheme 2).

The desired dense, face-to-face packing of **2** was revealed by the analysis of single crystals grown from $CDCl_3$ by slow solvent evaporation (Figure 1). **2** Crystallizes in the Sohncke group, $P2_1$. The absolute structure was not determined owing to a lack of resonant scatterers. The anthracene core and the cyano groups are virtually coplanar (maximum distance from the least squares (LS) plane defined by the C atoms of the anthracene: 0.0885(19) Å for N2). The nitro groups, in contrast, are distinctly twisted (maximum distance from the LS plane: 0.4475(19) for O4). The molecules are connected by

DOI: 10.1021/acsomega.7b00245
ACS Omega 2017, 2, 1594–1600

$\pi-\pi$ interactions to rods extending along [100] with a distance of 3.417 Å (Figure 1C). The rods connect through the cyano and nitro groups to the layers in the [010] direction; these layers are connected by the nitro groups in the [001] direction (LS planes inclined by 32.7°) (Figure 1D).

In an effort to grow larger single crystals of **2**, acetonitrile was found to be the best-suited solvent. Slow evaporation yielded single-crystalline, bright yellow, needlelike crystals of 30 to several hundred micrometers in diameter (Figure 2A) and up to 1 cm in length. The same crystal structure as from $CDCl_3$ was obtained. Scanning electron microscopy (SEM) evinces hexagonal cross sections (Figure 2E,F) and shows tapered ends (Figure 2D). Also, SEM clearly underlines the high quality of the single crystals. We do not find evidence for weathering; instead, the crystals show smooth facets and sharp edges.

As expected, orienting the crystals in the diffractometer confirmed that the π-stacking direction nicely aligns with the length axis of the needlelike crystals (see SI). The crystal morphology computed using the BFDH algorithm (Figure 2G–I) is in agreement with the crystal habit observed by microscopy. These insights allow for unambiguously determining the orientation of the molecules within the prismatic single crystals. As mentioned above, the orientation is important for applications in organic electronics (such as organic single-crystal transistors) because charge transport in organic materials preferentially occurs along the stacking direction.

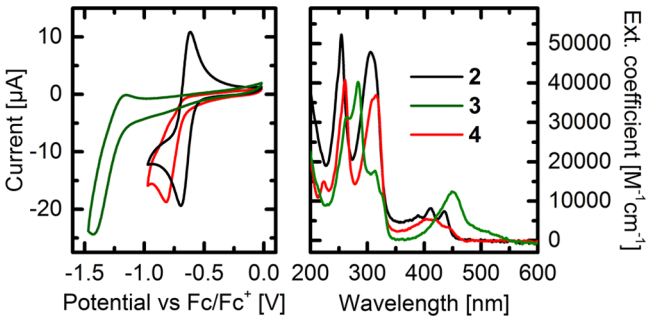

Figure 3. Cyclic voltammograms (left) and absorption spectra (right) of compounds **2**, **3**, and **4**. For the cyclic voltammograms, the ferrocene oxidation onset (Fc/Fc^+) was determined as the reference. All measurements were carried out in acetonitrile.

Table 1. Electrochemical Reduction Onset Potentials (E_{red}) and Optical Gaps (E_g^{opt}) Deduced from the Measurements in Figure 3[a]

compound	E_{red} [V][b]	E_g^{opt} [eV][c]	LUMO [eV][d]	HOMO [eV][e]
2	−0.58	2.75	−4.22	−6.97
3	−1.21	2.20	−3.59	−5.79
4	−0.67	2.67	−4.13	−6.80
DCA	−1.20	2.85	−3.60	−6.45

[a]HOMO and LUMO levels of compounds **2**, **3**, and **4** in comparison with those of DCA. [b]Versus ferrocene/ferrocene$^+$ (Fc/Fc^+). [c]Corresponding to the absorption onset. [d]Estimated on the premise that the Fc/Fc^+ energy level is −4.80 eV. [e]Determined by subtracting the optical gap energy from the LUMO level.

The LUMO levels of **2**, **3**, and **4** were determined by cyclic voltammetry (Figure 3, Table 1); DCA was measured for comparison (also see SI). Most interestingly, high reversibility was observed for the reduction of 2,7-dinitro-9,10-dicyanoanthracene **2**, whereas the reduction of the halogenated byproduct, **4**, was not reversible at all. The high reversibility of the reduction of dicyanoacenes was recently attributed to the delocalization of the resulting singly occupied molecular orbital and the electron spin density over the whole molecule.[19] This effect benefits the chemical stability of the negatively charged radical species and was shown to be valuable for applications in rechargeable batteries. The small reduction onset potential of **2** corresponds to a very low LUMO level of −4.22 eV. To the best of our knowledge, this is the lowest LUMO level of any anthracene derivative reported to date, significantly lower than the LUMO level of DCA and even lower than the LUMO level of the alkyl imide functionalized DCAs mentioned above.[14] The similarity to the LUMO levels of the cyanated pentacenes confirms the general strategy.

As expected, turning the electron-withdrawing nitro groups into electron-donating amino groups resulted in a higher LUMO level of **3**. However, the resulting push–pull system narrows the optical gap and limits this effect. While **3** is a promising building block for further chemical modifications, the very low LUMO level and the face-to-face stacking along the crystals' length axes render **2** most interesting for organic electronics (in particular for n-type organic transistors). For such applications, thermal stability is an issue and the nitro groups may raise concerns. Fortunately, thermogravimetric analysis revealed full stability of **2** up to 211 °C (see SI). Because **2** can be easily processed from solution and processing by thermal evaporation is not required, this is sufficient for most applications. Glass transition or melting has not been observed by differential scanning calorimetry (DSC) measuring up to 235 °C.

Anthracene derivatives are usually excellent fluorescence emitters, but ultrafast intersystem crossing (ISC) from the singlet into the triplet state was reported for nitroanthracenes.[20] As a consequence, fluorescence has not been observed for these compounds. Measurements of **2** confirmed the expected detrimental effect of the nitro groups on the fluorescence of DCA (see SI), which (without nitro groups) is an excellent fluorescence emitter.[10,21] Because ISC is a prerequisite for compounds to be used as photosensitizers, the application of **2** in photocatalysis is promising.

CONCLUSIONS

Rational molecular design of the target compound, 2,7-dinitro-9,10-dicyanoanthracene **2**, allowed for the material properties to be manipulated as desired. Increasing the number of EWGs resulted in, to the best of our knowledge, the lowest LUMO level measured for any anthracene derivative reported to date. Moreover, the careful selection of the substituents and substitution positions ensured face-to-face molecular packing and improved solubility. The packing results confirm that opposing cyano groups significantly strengthen face-to-face interactions of acenes.

For the synthesis of **2**, the reaction from quinones to cyanated acenes had to be adapted to allow for the conversion of 2,7-dinitro-9,10-anthraquinone **1**. The improved protocol, which is characterized by a delayed addition of the catalyst, is expected to be generally applicable to electron-poor starting materials. The synthesis had to be further improved for the preparation of **2** on a larger scale.

Brominated cyanoanthracene **4** was formed as a byproduct in the reaction toward **2**. The byproduct points the way for a synthesis of halogenated acenes from quinones by reductive aromatization. For the preparation of **2**, the formation of this

DOI: 10.1021/acsomega.7b00245
ACS Omega 2017, 2, 1594–1600

byproduct could be efficiently suppressed by the improved reaction conditions.

According to fluorescence measurements, **2** may be an interesting photosensitizer. Moreover, selective reduction of the nitro groups to amines was found to be feasible. Future applications of **2** in organic electronics are most exciting, considering the very low LUMO level, the face-to-face packing, the π-stacking direction aligning with the crystals' length axes, and the large single crystals obtained from solution.

EXPERIMENTAL SECTION

Reagents and solvents for all reactions were purchased from commercial suppliers and used without further purification, except for PBr_3, which was purified by distillation. Reactions were monitored by thin-layer chromatography (silica gel 60 F254; Merck). Column chromatography was performed using silica 60 (40−63 μm; Merck). Solubility data were obtained by sonicating an excess of compound **2** with 2 mL of solvent for 10 min at room temperature. The suspension was then filtered, and 1.5 mL of the resulting solution was used to determine the dissolved amount of **2** by evaporation of the solvent. NMR spectra were recorded at 600 MHz for ^{1}H and 150 MHz for ^{13}C on a Bruker Avance III HD spectrometer and at 400 MHz for ^{1}H on a Bruker Avance DRX-400 spectrometer. Data for ^{1}H NMR are reported as follows: chemical shift in parts per million (ppm) from tetramethylsilane (TMS) using the residual solvent signal as an internal reference ($CDCl_3$: δ = 7.26 ppm, DMSO-d_6: δ = 2.50 ppm), multiplicity (s = singlet, d = doublet, dd = doublet of doublets), and integration. ^{13}C NMR data are reported in ppm from TMS using the central peak of the solvent as reference ($CDCl_3$: δ = 77.16 ppm, DMSO-d_6: δ = 39.52 ppm); the multiplicity with respect to H (s = quaternary C, d = CH) is deduced from APT experiments. HPLC measurements were carried out on a system of Agilent Technologies (1200 Series G1367B HiP ALS Autosampler, 1100 Series G1311A Quat Pump, 1100 Series G1379A Degasser, 1200 Series G1316B TCCSL, 1260 Infinity G1315D DAD). Mobile phase: water (from 95 to 1%), acetonitrile (from 5 to 99%), formic acid (0.1%). Cyclic voltammetry measurements of **2**, **3**, and **4** were carried out using Metrohm Autolab B.V equipment (PGSTAT128N, differential electrometer amplifier). The measurements were performed at a scan rate of 0.05 V s^{-1} using 0.20 mM solutions in acetonitrile. Tetrabutylammonium tetrafluoroborate (n-Bu_4NBF_4, 0.1 M) was added to the solutions as the supporting electrolyte. The solutions were purged with nitrogen for 10 min before the measurements. A three-electrode configuration consisting of a platinum working electrode, a platinum counter electrode, and a silver chloride-coated silver reference electrode was used. Ferrocene (Fc) was measured as the reference material. The LUMO levels were deduced from the reduction onset potentials on the premise that the ferrocene oxidation onset (Fc/Fc^+) corresponds to an energy level of −4.80 eV. UV−vis absorption spectra were recorded at room temperature on a Thermo Scientific NanoDrop One^c spectrometer. The measurements were carried out using cuvettes filled with 5 μM sample solutions in acetonitrile. Fluorescence spectra were recorded at room temperature on a PerkinElmer LS 55 spectrometer. The measurements were carried out using 5 μM sample solutions in acetonitrile. Excitation wavelengths maximizing the fluorescence intensity at the emission maxima were determined by excitation scans (**2**: 340 nm, **3**: 450 nm, **4**: 315 nm; DCA: 400 nm). Other measurement parameters: ExSlit: 2.5; EmSlit: 2.5; detector voltage: 900 (high gain), 775 (medium gain), 650 (low gain). Thermogravimetric analysis was carried out under a flow of nitrogen at a heating rate of 10 K min^{-1} on a Netzsch TG 209, working with Al_2O_3 pans. DSC was carried out at a heating rate of 10 K min^{-1} under a flowing argon atmosphere on a Netsch DSC 200 F3 Maia, working with aluminum pans with pierced lids. Optical microscopy was performed on a LEICA M 125 microscope; images were taken using the software LAS v3.7. SEM was carried out with a Quanta 200F FEImicroscope. The samples were measured at 5 or 10 kV, with a working distance of 9−10 mm and a spot size of 2.0. Before imaging, samples were loaded on carbon-coated stubs and coated by sputtering with a 17-nm-thick layer of Au/Pd 60/40 alloy with a Quarum Q105T S sample preparation system. X-ray diffraction data of **2** and **4** (CCDC entries 1530990 and 1530991) were collected at T = 100 K in a dry stream of nitrogen on a Bruker Kappa APEX II diffractometer system using graphite-monochromatized Mo Kα radiation (λ = 0.71073 Å) and fine-sliced φ- and ω-scans. X-ray diffraction data were reduced to intensity values with SAINT, and an absorption correction was applied with the multiscan approach implemented in SADABS.[22] The structures were solved by dual-space methods implemented in SHELXT[23] and refined against F with JANA2006.[24] Nonhydrogen atoms were refined anisotropically. H atoms were placed in calculated positions and thereafter refined as riding on the parent C atoms. Molecular graphics were generated with the MERCURY program.[25]

2,7-Dinitro-9,10-anthraquinone (1). The synthesis followed the protocol reported by Perry et al.[18] Instead of standing at room temperature for 1 week, standing overnight was found to be sufficient. The final precipitate (after boiling in glacial acetic acid) was also filtered after standing overnight. Intensive washing of the solid with ethyl acetate (instead of glacial acetic acid and hexane) afforded **1** as a pale yellow powder (7.26 g, 34%). Purification by recrystallization was not required. ^{1}H NMR (400 MHz, DMSO-d_6, δ): 8.83 (d, J = 2.3 Hz, 2H), 8.71 (dd, J = 2.3, 8.6 Hz, 2H), 8.48 (d, J = 8.6 Hz, 2H) ppm (in accordance with the literature[18]). ^{1}H NMR (400 MHz, $CDCl_3$, δ): 9.19 (d, J = 2.3 Hz, 2H), 8.68 (dd, J = 2.3, 8.5 Hz, 2H), 8.58 (d, J = 8.5 Hz, 2H) ppm.

2,7-Dinitro-9,10-dicyanoanthracene (2). 2,7-Dinitro-9,10-anthraquinone **1** (1491 mg, 5.00 mmol, 1.00 equiv) was suspended in dry DMF (2.50 mL, 2.0 M) under an argon atmosphere in a 50 mL three-necked round-bottom flask (equipped with a septum and an argon balloon). The flask was cooled to 0 °C with an ice bath, TMSCN (1017 mg, 1.28 mL, 10.25 mmol, 2.05 equiv) was added, and the resulting mixture was stirred at 0 °C for 90 min. Note: Magnetic stirring is difficult at this stage. Adding larger amounts of DMF to solve this issue is not recommended; this affects the reductive aromatization after adding PBr_3. For reactions on a small scale, stirring with a stirring rod from time to time is recommended. For reactions on a larger scale, mechanical stirring is recommended as an alternative. KCN (16 mg, 0.25 mmol, 0.05 equiv) was then added, and the reaction was stirred for another 3 h at 0 °C. After slowly diluting with 15 mL of dry acetonitrile, PBr_3 (1624 mg, 0.56 mL, 6.00 mmol, 1.20 equiv) was added (still at 0 °C). The reaction was then placed in an ice-filled, covered dewar flask and stirred overnight. The resulting suspension, which warmed to 15 °C overnight, was diluted with 15 mL of CH_2Cl_2 and directly filtered over a thick pad of silica (conditioned with CH_2Cl_2 and some drops of acetonitrile) using CH_2Cl_2 as the eluent. After evaporation of

DOI: 10.1021/acsomega.7b00245
ACS Omega 2017, 2, 1594−1600

the solvent, the residue was purified by column chromatography (petroleum ether/CH_2Cl_2 3:2 → 1:1). Evaporation of the solvent afforded **2** (948 mg, 2.98 mmol, 60%) as a yellow solid. ^{1}H NMR (600 MHz, $CDCl_3$, δ): 9.52 (d, J = 2.1 Hz, 2H), 8.78 (d, J = 9.4 Hz, 2H), 8.69 (dd, J = 9.4, 2.1 Hz, 2H) ppm; ^{13}C NMR (150 MHz, $CDCl_3$, δ): 148.5 (s), 134.8 (s), 131.7 (s), 129.2 (d), 124.8 (d), 123.4 (d), 117.7 (s), 114.5 (s), 114.1 (s), 113.3 (s) ppm. λ^{max} (ε) = 254 (52 000), 306 (48 000), 411 (8000), 435 nm (7000 M^{-1} cm^{-1}). The molecular structure was confirmed by single-crystal X-ray diffraction. DSC did not evince melting up to the decomposition temperature.

2,7-Diamino-9,10-dicyanoanthracene (3). 2,7-Dinitro-9,10-dicyanoanthracene **2** (382 mg, 1.20 mmol, 1.0 equiv) and $SnCl_2 \cdot 2H_2O$ (2166 mg, 9.60 mmol, 8.0 equiv) were suspended in 12 mL of EtOH (0.1 M) and heated to reflux for 4 h with an oil bath. The solvent was then evaporated in vacuo, and the solid residue was transferred into a separating funnel with ethyl acetate and saturated aqueous $NaHCO_3$. The mixture was extracted with 2 × 200 mL and 2 × 100 mL of ethyl acetate, and the combined organic layers were dried over sodium sulfate. Evaporation of the solvent afforded **3** (260 mg, 1.01 mmol, 84%) as a dark red solid. ^{1}H NMR (600 MHz, DMSO-d_6, δ): 7.95 (d, J = 9.1 Hz, 2H), 7.18 (dd, J = 9.1, 2.1 Hz, 2H), 7.03 (d, J = 2.1 Hz, 2H), 6.52 (s, 4H) ppm; ^{13}C NMR (150 MHz, DMSO-d_6): 150.4 (s), 135.7 (s), 127.0 (d), 122.6 (s), 121.7 (d), 118.1 (s), 116.3 (s), 110.0 (s), 98.9 (d), 96.9 (s) ppm. λ^{max} (ε) = 284 (40 000), 450 nm (12 000 M^{-1} cm^{-1}). HRMS (ESI) m/z: $[M]^+$ Calcd for $C_{16}H_{10}N_4$ 258.0900; Found 258.0902; $[M + H]^+$ Calcd for $C_{16}H_{11}N_4$ 259.0978; Found 259.0993 $[M + H]^+$. DSC did not evince melting up to the decomposition temperature.

2,7-Dinitro-9-bromo-10-cyanoanthracene (4). 2,7-Dinitro-9,10-anthraquinone **1** (1491 mg, 5.00 mmol, 1.00 equiv) was suspended in dry DMF (2.50 mL, 2.0 M) in a 50 mL three-necked round-bottom flask (equipped with a septum and an argon balloon). TMSCN (1017 mg, 1.28 mL, 10.25 mmol, 2.05 equiv) was added at room temperature, and the resulting mixture was stirred for 1 h. KCN (16 mg, 0.25 mmol, 0.05 equiv) was then added, and the reaction was stirred for another 90 min. After diluting with 15 mL of dry acetonitrile, PBr_3 (1624 mg, 0.56 mL, 6.00 mmol, 1.20 equiv) was added, and the reaction was stirred at room temperature for 3 h. The resulting suspension was filtered, and the solid was washed with acetonitrile and subjected to column chromatography (petroleum ether/CH_2Cl_2 3:2 → 1:1), which afforded pure compound **4** as a yellow solid (128 mg, 0.34 mmol, 7%) and a mixture (588 mg) of starting material **1** (0.39 mol %; calculated: 219 mg, 0.73 mmol, 15%), **2** (0.57 mol %; calculated: 341 mg, 1.07 mmol, 21%), and **4** (0.04 mol %; calculated: 28 mg, 0.08 mmol, 2%) (mole fractions according to ^{1}H NMR). Characterization data of **4**: ^{1}H NMR (600 MHz, $CDCl_3$, δ): 9.67 (d, J = 2.1 Hz, 2H), 8.69 (d, J = 9.4 Hz, 2H), 8.60 (dd, J = 9.4, 2.1 Hz, 2H) ppm; ^{13}C NMR (150 MHz, $CDCl_3$, δ): 147.7 (s), 136.6 (s), 136.0 (s), 130.2 (s), 128.9 (d), 126.6 (d), 124.2 (d), 115.4 (s), 108.3 (s) ppm. λ^{max} (ε) = 260 (41 000), 315 (37 000), 405 nm (5000 M^{-1} cm^{-1}). The molecular structure was confirmed by single-crystal X-ray diffraction.

■ ASSOCIATED CONTENT

Supporting Information

The Supporting Information is available free of charge on the ACS Publications website at DOI: 10.1021/acsomega.7b00245.

^{1}H and ^{13}C(APT) NMR spectra of all new compounds, cyclic voltammograms, UV−vis absorption spectra, fluorescence spectra, thermogravimetric analysis, details for X-ray structure determination, HPLC measurements (PDF)

Data for 2,7-dinitro-9,10-dicyanoanthracene and 2,7-dinitro-9-bromo-10-cyanoanthracene (CIF)

■ AUTHOR INFORMATION

Corresponding Author

*E-mail: florian.gloecklhofer@tuwien.ac.at.

ORCID

Florian Glöcklhofer: 0000-0002-6911-8563

Notes

The authors declare no competing financial interest.

■ ACKNOWLEDGMENTS

We gratefully thank Manuel Spettel for contributing to synthetic experiments, Christian Hametner for NMR measurements, Stefan Lexmüller and Julia Weber for HPLC measurements, Lukas Leimhofer for thermogravimetric analysis, and Paul Kautny for DSC. The X-ray center and the interfaculty electron microscopy facility (USTEM) of the TU Wien are acknowledged for providing access to the single-crystal diffractometer and to the scanning electron microscope. The authors acknowledge the TU Wien University Library for financial support through its Open Access Funding Program.

■ REFERENCES

(1) Zhou, K.; Dong, H.; Zhang, H.-l.; Hu, W. *Phys. Chem. Chem. Phys.* **2014**, *16*, 22448−22457.

(2) Yun, S. W.; Kim, J. H.; Shin, S.; Yang, H.; An, B.-K.; Yang, L.; Park, S. Y. *Adv. Mater.* **2012**, *24*, 911−915.

(3) Stolar, M.; Baumgartner, T. *Phys. Chem. Chem. Phys.* **2013**, *15*, 9007−9024.

(4) Glöcklhofer, F.; Lunzer, M.; Stöger, B.; Fröhlich, J. *Chem. - Eur. J.* **2016**, *22*, 5173−5180.

(5) Katsuta, S.; Miyagi, D.; Yamada, H.; Okujima, T.; Mori, S.; Nakayama, K.-i.; Uno, H. *Org. Lett.* **2011**, *13*, 1454−1457.

(6) Li, A.; Wen, S.-H.; Song, J.-L.; Deng, W.-Q. *Org. Electron.* **2009**, *10*, 1054−1059.

(7) Glöcklhofer, F.; Petritz, A.; Karner, E.; Bojdys, M. J.; Stadlober, B.; Fröhlich, J.; Unterlass, M. M. *J. Mater. Chem. C* **2017**, *5*, 2603−2610.

(8) Wang, C.; Dong, H.; Hu, W.; Liu, Y.; Zhu, D. *Chem. Rev.* **2012**, *112*, 2208−2267.

(9) Glöcklhofer, F.; Lunzer, M.; Fröhlich, J. *Synlett* **2015**, *26*, 950−952.

(10) Glöcklhofer, F.; Kautny, P.; Fritz, P.; Stöger, B.; Fröhlich, J. *ChemPhotoChem* **2017**, *1*, 51−55.

(11) Anthony, J. E. *Angew. Chem., Int. Ed.* **2008**, *47*, 452−483.

(12) Anthony, J. E.; Facchetti, A.; Heeney, M.; Marder, S. R.; Zhan, X. *Adv. Mater.* **2010**, *22*, 3876−3892.

(13) Akar, K. B.; Çakmak, O. *Tetrahedron Lett.* **2013**, *54*, 312−314.

(14) Usta, H.; Kim, C.; Wang, Z.; Lu, S.; Huang, H.; Facchetti, A.; Marks, T. J. *J. Mater. Chem.* **2012**, *22*, 4459−4472.

(15) Cheng, Y.-J.; Yang, S.-H.; Hsu, C.-S. *Chem. Rev.* **2009**, *109*, 5868−5923.

(16) Exner, O.; Krygowski, T. M. *Chem. Soc. Rev.* **1996**, *25*, 71−75.

(17) Pinal, R. *Org. Biomol. Chem.* **2004**, *2*, 2692−2699.

(18) Perry, P. J.; Reszka, A. P.; Wood, A. A.; Read, M. A.; Gowan, S. M.; Dosanjh, H. S.; Trent, J. O.; Jenkins, T. C.; Kelland, L. R.; Neidle, S. *J. Med. Chem.* **1998**, *41*, 4873−4884.

(19) Deng, Q.; He, S.-J.; Pei, J.; Fan, C.; Li, C.; Cao, B.; Lu, Z.-H.; Li, J. *Electrochem. Commun.* **2017**, *75*, 29−32.

DOI: 10.1021/acsomega.7b00245
ACS Omega 2017, 2, 1594−1600

(20) Hamanoue, K.; Hirayama, S.; Nakayama, T.; Teranishi, H. *J. Phys. Chem.* **1980**, *84*, 2074−2078.
(21) Schoof, S.; Güsten, H.; Von Sonntag, C. *Ber. Bunsen.-Ges.* **1978**, *82*, 1068−1073.
(22) *Bruker, APEX2, SAINT and SADABS*; Bruker AXS Inc.: Madison, Wisconsin, 2015.
(23) Sheldrick, G. M. *Acta Crystallogr., Sect. A: Found. Adv.* **2015**, *71*, 3−8.
(24) Petříček, V.; Dušek, M.; Palatinus, L. *Z. Kristallogr. - Cryst. Mater.* **2014**, *229*, 345−352.
(25) Macrae, C. F.; Edgington, P. R.; McCabe, P.; Pidcock, E.; Shields, G. P.; Taylor, R.; Towler, M.; van de Streek, J. *J. Appl. Crystallogr.* **2006**, *39*, 453−457.

DOI: 10.1021/acsomega.7b00245
ACS Omega 2017, 2, 1594−1600